Predicting Adsorption Equilibrium Using Molecular Simulation

Graham M. Davies
Dept. of Chemical Engineering, University of Cambridge, Pembroke Street, Cambridge, CB2 3RA, U.K.

Nigel A. Seaton
School of Chemical Engineering, University of Edinburgh, King's Buildings, Mayfield Road, Edinburgh, EH9 3JL, U.K.

The capability of molecular simulation, combined with pore-size distribution (PSD) analysis, to predict adsorption equilibrium in microporous carbon adsorbents, using as a case study the adsorption of methane and ethane, was investigated. The calculations indicate that a wide range of data for the adsorption of pure components and binary mixtures can be predicted successfully. Significantly, only a limited set of experimental data comprising three or four adsorption measurements is required to calculate the PSD. This predictive ability is relevant to both the design of adsorptive separation processes and the design of new adsorbents.

Introduction

Classical thermodynamic methods such as ideal adsorbed solution theory (IAST) (Myers and Prausnitz, 1965) are used widely in industry to predict the adsorption equilibrium of gas mixtures. However, employing these techniques requires a substantial amount of experimental data. For example, even the most straightforward IAST prediction requires pure-component isotherms at the temperature at which the prediction is to be made, for all the components in the mixture. This places a considerable burden on the designer of an adsorptive separation process, compared with more conventional separation techniques, such as distillation. Another disadvantage of these techniques is related to the inherent confidence that we are able to place in the predictions. Although IAST and kindred thermodynamic methods often yield accurate predictions, they do on occasion fail catastrophically, even for supposedly ''thermodynamically ideal'' systems [see, for example, Gusev et al. (1996)], and, as we will show, the data requirements to identify when this is likely to occur are severe. A third limitation of classic thermodynamic models is that they cannot be used to design *adsorbents*. In the adsorbent design problem, a method is required to predict pure and multicomponent adsorption on the basis of the physical structure and chemical composition of the adsorbent. Such a method could be applied to improve existing adsorbents and to engineer ''designer'' adsorbents—adsorbents that are tailor-made for a specific application. Examples of designer adsorbents would include an activated carbon that is synthesized to yield a predetermined pore-size distribution or a zeolite that is synthesized to include a particular type or distribution of cations. In each case, the adsorbent is synthesized to include a predetermined set of desirable attributes. Clearly, as one cannot obtain experimental data on the adsorbent before it is synthesized, thermodynamic models such as IAST cannot be used to determine the best attributes to aim for during synthesis.

In this article we investigate the capability of a molecular simulation method, grand canonical Monte Carlo (GCMC) simulation, used in conjunction with a pore-size distribution (PSD) analysis to predict adsorption equilibrium. This statistical–mechanical approach makes a direct connection between a physical description of adsorption at the molecular and pore levels, and the macroscopic adsorption behavior. Because it accounts directly for the effect of pore structure on adsorption equilibrium, the GCMC/PSD method is much less dependent than classic thermodynamic methods on experimental data, needing only enough data to characterize the adsorbent, or, for the adsorbent design problem, a structural description of a hypothetical adsorbent.

Correspondence concerning this article should be addressed to N. A. Seaton.

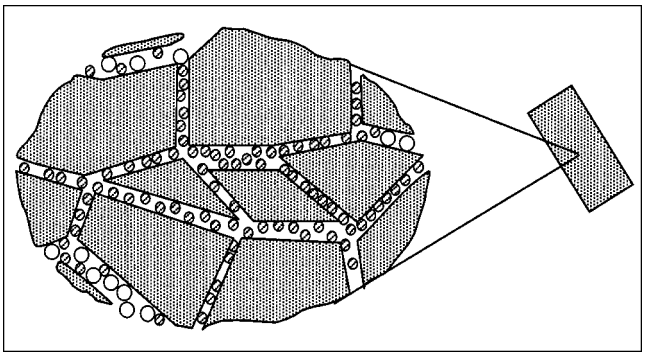

Figure 1. 2-D network of model pores.

Characterizing the adsorbent therefore involves identifying and quantifying the most important attributes of the adsorbent that affect the adsorption of gases onto it. We have found (Davies and Seaton, 1999) that in many instances a pore network model of the internal structure of the adsorbent is able to account for a large range of adsorption data. In a pore network model, shown in two dimensions in Figure 1, pores of various widths are connected together to form a network. Provided that the pores are sufficiently long, the pore junctions make only a small contribution to adsorption. Therefore, the two important factors that affect adsorption in this model are the pore-size distribution (PSD), and the connectivity of the pore network. The PSD affects adsorption because gases adsorb to differing extents in pores of different pore widths. The connectivity of the pore network (that is, the way the pores are connected together) in turn influences adsorption by limiting the accessibility of some components to regions of the network. Depending on the PSD, some components might be so large that they cannot enter all the pores. For a network of sufficiently low coordination number, this molecular sieving effect can extend to clusters of pores, including some that are large enough for all the components to enter, but that are isolated by the presence of constrictions elsewhere in the pore network; molecular sieving is then a percolation problem (López-Ramón et al., 1997; Davies and Seaton, 1999). We assume, for the moment, that the coordination number of the pore network is sufficiently large that all the adsorptive species have access to the entire pore network. In other words, at this stage we assume that the behavior of the adsorbent can be characterized in terms of the PSD, $f(w)$, which is calculated from the adsorption integral equation:

$$N_s(T, P, y)_i = \int_0^\infty \rho_{mp,s}(w, T, P, y)_i f(w)\, dw \qquad i = 1 \cdots n, \tag{1}$$

where $N_s(T, P, y)_i$ is the adsorption of component s at temperature T, bulk fluid phase pressure P, and composition y; $\rho_{mp,s}(w, T, P, y)_i$ is the "model-pore isotherm," that is, the density of adsorptive in a model pore of width, w, calculated using GCMC simulation, and n is the number of adsorption measurements used in the analysis.

In this article, Eq. 1 is used in two modes: characterization and prediction. First the adsorbent is characterized by fitting the PSD to experimental data. Adsorption is then predicted under other conditions (at a different temperature, pressure, or composition) using this PSD. Thus, in solving Eq. 1 in characterization mode, $N_s(T, P, y)_i$ is known and $f(w)$ unknown, while in prediction mode, $f(w)$ is known and $N_s(T, P, y)_i$ unknown.

Two difficulties arise in calculating a PSD from Eq. 1: this equation is both ill-posed and ill-conditioned. Ill-posedness means that there may be several, possibly quite dissimilar PSDs that are consistent, to within a small margin of error, with the experimental data. The ill-conditioning in turn refers to the fact that small perturbations in the experimental data might lead to substantial differences in the calculated PSDs (Davies et al., 1999). The fact that several markedly distinct PSDs can usually be calculated from a set of experimental data (each consistent with the data) raises the following question: If these PSDs are used to predict adsorption under different conditions, will the predictions based on these different PSDs be similar to one another? To pose the problem in mathematical terms, the ill-posed and ill-conditioned character of the adsorption integral equation (Eq. 1) means that one set of experimental adsorption data maps to more than one PSD; we need to ascertain whether the many PSDs map to similar predictions for all pure-component and multicomponent adsorption in which we are interested. In practice, the question is whether the predictions are sufficiently close to each other for engineering purposes. This is illustrated in Figure 2, which shows two PSDs for Nuxit activated carbon that are consistent with the adsorption of methane at 293 K; to within a small margin of error, the methane isotherm can be mapped onto two quite dissimilar PSDs (that is, a one-to-many mapping). The "small margin of error" refers to the minor differences in the fit to the methane data, which are also shown in Figure 2. Also shown in this figure are the predicted extents of ethane adsorption at 293 K. The predictions were made using Eq. 1, the PSD determined from the methane adsorption isotherm, and a set of model-pore isotherms for ethane adsorption at 293 K. We term this approach a GCMC/PSD prediction. Of the two PSDs, only one is capable of predicting the ethane adsorption accurately over a wide range of pressure; the mapping from the PSD to the ethane adsorption is not close to a many-to-one mapping. We therefore either require tools to differentiate between the two PSDs or to determine their ranges of validity with respect to predicted extents of adsorption.

A more fundamental problem also exists, related to the amount and type of experimental data that is required to calculate a PSD. In using Eq. 1 we made two tacit assumptions. The first assumption was that a PSD exists that is consistent with a wide range of adsorption data: the data from which the PSD is to be calculated as well as the data that we wish to predict. The second assumption was that this PSD could be calculated from a limited amount of adsorption data.

The assumption that a consistent PSD exists is ultimately related to the realism of the PSD analysis. In other words, if the dominant attribute of the internal structure affecting adsorption is indeed the pore width (that is, the proximity of adsorbing surfaces to each other) and not, for example, chemical heterogeneity, surface roughness, or the presence

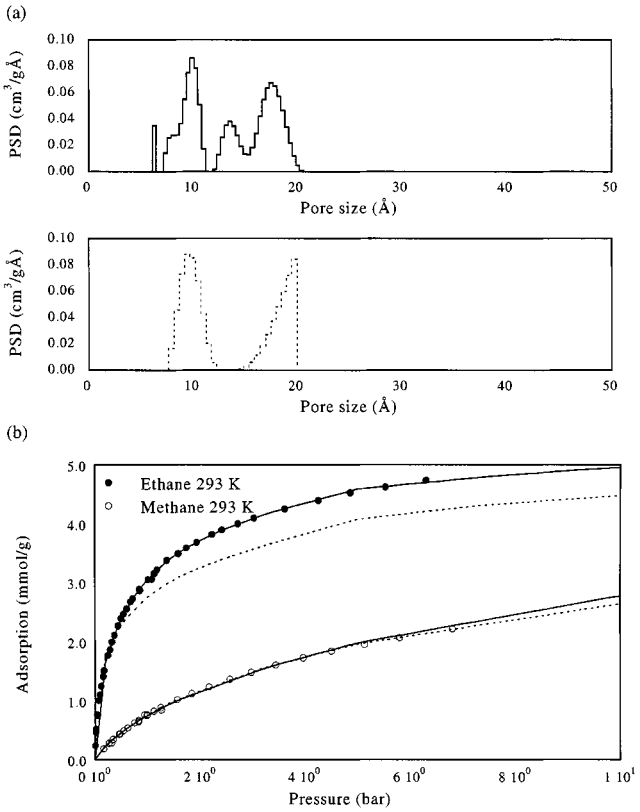

Figure 2. Ill-posed nature of the adsorption integral equation.

(a) Two PSDs consistent with the methane adsorption data shown in (b). (b) The fit to the methane data used to calculate the PSDs shown in (a) and the predicted extents of ethane adsorption based on these PSDs.

of constrictions in the pore network, we can reasonably expect a PSD to exist that is consistent with a wide range of adsorption data. If, however, another property of the adsorbent significantly affects adsorption, it is much less likely that a conventional PSD will be consistent with a wide range of data. Such a PSD might nevertheless be capable of fitting a limited range of data, such as those conventionally used in a characterization analysis—data for the adsorption of a single component at a single temperature. Therefore, the fitting of a single adsorption isotherm cannot by itself be taken as proof of the realism of the PSD analysis.

We have previously evaluated the realism of the PSD characterization by determining whether at least one PSD could be calculated that is consistent with a wide range of pure and multicomponent methane and ethane adsorption data for each of four commercially available activated carbons (Davies and Seaton, 1999). This was achieved by attempting to calculate a PSD based on all the available methane and ethane adsorption data simultaneously. Good agreement was found for three activated carbons. Significantly, however, we found that one of the activated carbons investigated, BPL, could not be characterized in terms of a PSD based on all the pure and binary methane and ethane adsorption data of Gusev and O'Brien (1997), although a significant improvement was made by taking into account pore network connectivity. Since these data correspond to typical operating conditions for an adsorptive separation unit, we were able to conclude that a conventional GCMC/PSD analysis is of limited value when designing separation units that employ BPL activated carbon, at least for mixtures of light hydrocarbons. It is worth noting three points related to this conclusion. First, this limitation is not specific to the GCMC/PSD analysis; IAST is also incapable of predicting binary adsorption onto BPL (Gusev et al., 1996). Second, as will be demonstrated later in this article, even for carbons such as BPL, the GCMC/PSD method has an advantage over the classic thermodynamic methods in that it can be systematically improved by incorporating additional information on the pore structure. Third, we have shown previously (Davies and Seaton, 1999) that when the PSD alone is identified as being an incomplete characterization of the pore structure, then there is little value in attempting to characterize such an activated carbon using a more limited set of data. This is because even if an excellent fit to the limited set of data could be achieved, as in the case of Gusev et al. (1997) and Gusev and O'Brien (1997), this fit is achieved at the expense of the agreement with the remaining data.

A more encouraging conclusion from this earlier investigation (Davies and Seaton, 1999), from the point of view of developing better tools to predict adsorption, was that consistent PSDs could be calculated based on pure and binary methane and ethane data for the remaining three activated carbons: Nuxit, AC40, and AK activated carbons. For these activated carbons at least, we are therefore now in a position to address the second tacit assumption in the characterization of adsorbents that we identified earlier—that a "suitable" characterization can be calculated from a limited amount of data. In the context of predicting adsorption, a "suitable" characterization is one that would yield accurate predictions using the GCMC/PSD approach. We therefore now specifically address the problem of determining the amount and type of data that is required to characterize the internal structure of an activated carbon such that the resulting characterization can be used to predict adsorption. As will become apparent, this investigation implicitly addresses the problem of identifying the most suitable PSDs on which to base predictions and of establishing the range of validity of a given PSD. This significantly improves our ability to evaluate adsorbents for proposed industrial applications and, as will be discussed in the penultimate section, facilitates the design of improved adsorbents.

The following two sections of the article present a brief summary of the calculation of adsorption in model pores using GCMC simulation and the determination of the PSD. In the fourth section we investigate whether a PSD that is calculated from a limited amount of adsorption data, such as a single pure-component isotherm, can be used to predict pure-component adsorption under other conditions, and multicomponent adsorption. This is followed in the fifth section by an investigation of the utility of calculating PSDs based on more than a single pure-component isotherm. This section also compares the performance of predictions based on PSDs and molecular simulation directly to the predominant classical technique used in industry, IAST (Myers and Prausnitz, 1965). The sixth section then considers the potential of using the GCMC/PSD approach as a tool for the design of improved adsorbents.

Molecular Simulation of Adsorption in Model Pores

Monte Carlo simulation is a stochastic method in which molecular configurations consistent with a given set of macroscopic variables are sampled, using rules that come from statistical mechanical theory. In the grand canonical ensemble, that is, the ensemble used in GCMC simulations, the specified macroscopic variables are the temperature, the chemical potentials of the adsorptive species, and the pore volume. (In practice, rather than specifying the chemical potentials directly in a simulation, it is preferable to specify measurable properties of the bulk-gas phase—the temperature, pressure, and composition. The simulation then employs a suitable equation of state to calculate the chemical potential of the adsorptives.) The outputs of a GCMC simulation include detailed information about the configurations adopted by adsorptive molecules in the pore and various thermodynamic properties. In the present context, the output information of interest is the amount and composition of the adsorbed phase in pores of various sizes, as a function of the temperature, pressure, and composition of the bulk gas phase, that is, the model-pore isotherm, $\rho_{mp,s}(w, T, P, y)_i$, in Eq. 1.

GCMC algorithms, and in some instances fragments of the actual source codes, have been well documented in the literature (see, for example, Nicholson and Parsonage, 1982; Allen and Tildesley, 1987; Frenkel and Smit, 1996). Alternatively, the adsorption in the model pores can be calculated using commercially available GCMC simulation packages. In this work, our own code was used. Here, we give only a brief outline of the simulation method.

The following input data are required, in addition to the thermodynamic state:

1. Suitable interaction potentials for the adsorptive and the adsorbent;
2. The potential cutoff distance, beyond which molecular interactions are ignored;
3. The pore width, and the other dimensions of the simulation cell;
4. The number of equilibration steps to be carried out in order to eliminate the effect of the initial (nonequilibrium) molecular configuration;
5. The number of steps over which output variables are to be calculated, after equilibration is complete.

In this work we have modeled methane as a single-site ''united atom'' and ethane as a two-site molecule. Since each of these sites can be treated as being nearly spherical and nonpolar, we have employed the Lennard-Jones interaction potential with the parameters for methane and ethane that are summarized in Table 1. To model the interaction between a site on an adsorptive molecule and a single semi-infinite pore wall of graphite, we employed the standard Steele 10-4-3 potential (Steele, 1974). The parameters for this potential are also summarized in Table 1. The potential cutoff used in this work was 17.145 Å, which is 4.5 times the Lennard-Jones diameter of methane.

The volume of the system is specified in terms of the dimensions of a so-called simulation cell. Since we have simulated adsorption in semi-infinite slit-shaped model pores, we adopted a standard rectangular simulation cell, the upper and lower surfaces of which represented the pore walls. The distance between these two surfaces, which was taken to be the z-dimension of the simulation cell, therefore defines the pore width. Although the simulations approximate a semi-infinite pore by employing periodic boundary conditions in the x- and y-direction, suitable dimensions of the simulation cell in these directions still need to be specified. We used x- and y-dimensions of 38.1 Å.

Table 1. Adsorbate and Adsorbent Parameters*

Parameters	Value
Methane parameters	
σ_{MM}	3.81 Å
ϵ_{MM}/k_B	148.2 K
Ethane parameters	
σ_{EE}	3.512 Å
ϵ_{EE}/k_B	139.8 K
Bond length	2.353 Å
Adsorbent parameters	
σ_{CC}	3.4 Å
ϵ_{CC}/k_B	28.0 K
Δ	3.35 Å
ρ_c	0.114 Å^{-3}

*Methane parameters from Hirschfelder et al. (1954); ethane parameters from Cracknell et al. (1994); adsorbent parameters from Steele (1974); k_B is the Boltzmann constant.

The chemical potentials of the adsorptive species were calculated from the specified temperature, pressure, and bulk gas composition using the Peng-Robinson equation of state.

The system was allowed to equilibrate for between 2×10^5 and 1×10^6 steps, and the properties were then calculated for between 1×10^6 and 5×10^6 steps.

Due to a subtle difference between simulated and experimentally determined extents of adsorption, simulated adsorption, termed absolute adsorption, needs to be transformed to a form that is commensurate with experimental measurements, which is termed excess adsorption. The simulated extents of adsorption used in this work were transformed to excess adsorption, $\rho_{mp,s}(w, T, P, y)_i$, using the method proposed by Davies and Seaton (1999).

Calculating the Pore-Size Distribution

Davies et al. (1999) and Davies and Seaton (1999) have recently addressed in detail the problem of calculating PSDs from adsorption data. We therefore present here only the most important aspects of the solution procedure. First, it is most convenient to employ a discrete representation of the PSD. When attempting to calculate a statistically significant PSD for an adsorbent, the number of quadrature intervals used in the analysis, m, must be less than or equal to the number of data points, n. The more quadrature intervals used in the analysis (and hence the more data), the smaller each quadrature interval will be and therefore the higher the resolution of the PSD.

The resolution of a PSD can also be improved by first identifying the range of pore sizes that can be characterized reliably from a given set of data and then assigning all but one of the quadrature intervals to this range. Gusev et al. (1997) recognized that for a given set of data, there is a maxi-

mum pore size that can identified reliably in a PSD analysis. Differentiating large pores from one another is difficult because the extent of adsorption (and in the case of mixtures, the selectivity) is virtually indistinguishable from one pore to another. This arises when the adsorption onto the opposite walls of a single pore occurs essentially independently (that is, the pore walls become too far away from each other to enhance adsorption). The pore size above which this occurs depends on the adsorptive (that is, the strength of the interaction between the adsorptive and atoms in the pore wall), and is a function of the temperature and the pressure. Gusev et al. (1997) therefore introduced the concept of a ''window of reliability'' into PSD analyses. This ''window'' extends from the smallest pore that the adsorptive can enter to the largest pore that can be reliably distinguished from the next largest pore. Since the adsorption in all the pores larger than those in the window of reliability is essentially indistinguishable, assigning a single quadrature interval to this region makes best use of the experimental data (Davies et al., 1999).

Adopting the suggested quadrature scheme, Eq. 1 can be approximated as

$$N_s(T,P,y)_i \approx \sum_{j=1}^{m} \rho_{mp,s}\left(w_j^*,T,P,y\right)_i f(w_j^*)\,\delta w_j, \quad (2)$$

where m is the number of quadrature intervals used in the analysis, with $m-1$ equally sized quadrature intervals lying within the window of reliability and one quadrature interval accounting for the adsorption in all the pores larger than those within the window of reliability, and w_j^* is the midpoint of each quadrature interval.

Equation 2 (or equivalently, Eq. 1) cannot be solved directly due to the ill-posed and ill-conditioned properties of these equations. The detrimental affect of both of these properties can, however, be minimized by employing regularization. Regularization, which has been described in detail by Wilson (1992), Von Szombathely et al. (1992), Merz (1980), and Whaba (1982), incorporates a measure of the overall smoothness of the PSD into the analysis. Physically, this corresponds to recognizing that a real PSD is more likely to be relatively smooth and centered around a few dominant pore sizes rather than highly fragmented and spiky. Adopting the square of the second derivative of the PSD as a suitable measure of its smoothness, the PSD is calculated by minimizing the residual defined by

$$R_{\mathrm{Reg}} = \sum_{i=1}^{n}\left[N_s(T,P,y)_i - \sum_{j=1}^{m} \rho_{mp,s}\left(w_j^*,T,P,y\right)_i \delta w_j f(w_j^*)\right]^2 + \alpha \sum_{j=1}^{m} f''(w_j^*)^2\,\delta w_j, \quad (3)$$

Table 2. Adsorption Data onto the Four Activated Carbons

Reference	Type of Activated Carbon	Adsorptive Species	Temp. (K)	Max. Press. (bar)	Window of Reliability (Å)
Szepesy and Illes (1963a,b,c)	Nuxit	Ethane	293	6.3	6.1− ~ 30
		Ethane	313	6.6	6.1− ~ 28
		Ethane	333	6.8	6.1− ~ 24
		Ethane	363	6.2	6.1− ~ 24
		Methane	293	6.8	6.1− ~ 20
		Methane	313	6.0	6.1− ~ 18
		Methane	333	4.9	6.1− ~ 18
		Methane	363	6.4	6.1− ~ 18
		Binary mixtures methane/ethane	293	1.0	
Costa et al. (1981)	AC40	Ethane	293	1.0	6.1− ~ 20
		Methane	293	1.0	6.1− ~ 16
		Binary mixtures methane/ethane	293	0.1	
Richter et al. (1989)	AK	Ethane	303	20.0	6.1− ~ 38
		Methane	303	20.0	6.1− ~ 22
		Binary mixtures methane/ethane	303	5	
		Binary mixtures methane/ethane	303	20	
Gusev and O'Brien (1997)	BPL	Ethane	308	29.9	6.1− ~ 42
		Ethane	333	29.8	6.1− ~ 38
		Ethane	373	30.4	6.1− ~ 30
		Methane	308	31.9	6.1− ~ 22
		Methane	333	31.9	6.1− ~ 22
		Methane	373	30.0	6.1− ~ 20
		Binary mixtures methane/ethane	308 333 373		

where $f''(w_j^*)$ is the second derivative of the PSD evaluated at w_j^* and α is a strictly nonnegative smoothing parameter.

One complicating factor in employing regularization is that it requires the identification of an optimal smoothing parameter to be used in the analysis. As in our previous work (Davies et al., 1999; Davies and Seaton, 1999), we have used generalized cross validation (GCV) and L curves to determine the optimal amount of smoothing.

Pore-size distributions can thus be calculated using Eq. 3, a given set of experimental adsorption data, such as one or more adsorption isotherms, and a set of simulated model-pore isotherms that correspond to the conditions of the data points. For example, we could envisage calculating a PSD based on an ethane isotherm at 293 K. This would necessarily require a set of model-pore isotherms for ethane at 293 K and the minimization of Eq. 3 for a range of smoothing parameters. The most representative PSD based on these data would then be the PSD that corresponds to the optimal extent of smoothing, which is identified using generalized cross validation and an L curve.

Predicting Adsorption Based on Experimental Adsorption Data for a Single Component

We initially investigated whether a PSD that is based on a single pure-component adsorption isotherm could be used to predict a range of pure-component and multicomponent adsorption. [This corresponds to the conventional approach to the characterization of porous solids using adsorption (Gregg and Sing, 1982), in which a single pure-component isotherm, typically for a standard adsorptive such as nitrogen or carbon dioxide, is used.] Table 2 summarizes the pure-component and binary methane and ethane adsorption data onto the three activated carbons that have been used in this investigation. [The fourth carbon studied, BPL, presented difficulties in the earlier PSD analysis (Davies and Seaton, 1999), and also requires special treatment in the predictive mode. This adsorbent is therefore addressed in the next section.] Also shown in this table is an estimate of the window of reliability, determined using the procedure suggested by Gusev et al. (1997), for each of the pure-component isotherms. In order to calculate a PSD for each activated carbon that spanned the largest range of pore sizes based on a single adsorption isotherm, we initially calculated the PSD for each activated carbon based on the isotherm with the widest window of reliability. The upper limit of the window of reliability is largest for the most strongly adsorbing component at the lowest temperature available—ethane at 293 K for the Nuxit and AC40, and ethane at 303 K for the AK activated carbon. These PSDs, their corresponding fits to the data used to calculate them and predictions of adsorption that are based on them are presented in Figures 3 to 11. These figures clearly demonstrate that not only can PSDs be fitted closely to a pure-component ethane adsorption isotherm, but also that the resulting PSD can then be used with remarkable success to predict

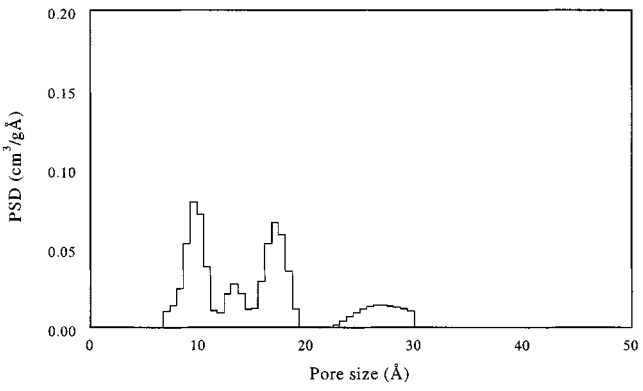

Figure 3. PSD for Nuxit activated carbon based on the adsorption of ethane at 293 K.

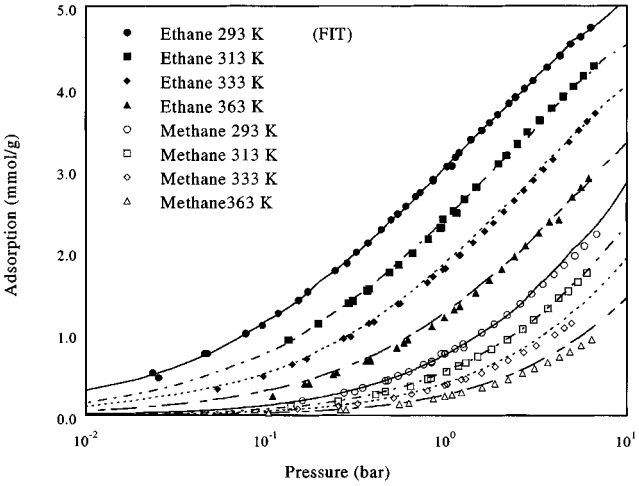

Figure 4. Predicted adsorption of ethane at 313, 333 and 363 K and methane at 293, 313, 333 and 363 K onto Nuxit activated carbon based on PSD in Figure 3 vs. experimental data.

Also shown is the fit to the ethane adsorption data at 293 K that was used to calculate the PSD.

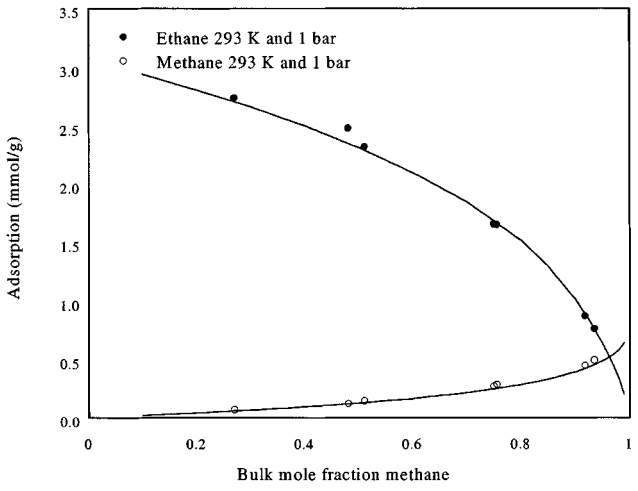

Figure 5. Predicted adsorption from bulk fluid mixtures at 293 K and 1 bar onto Nuxit activated carbon based on PSD in Figure 3 vs. experimental data.

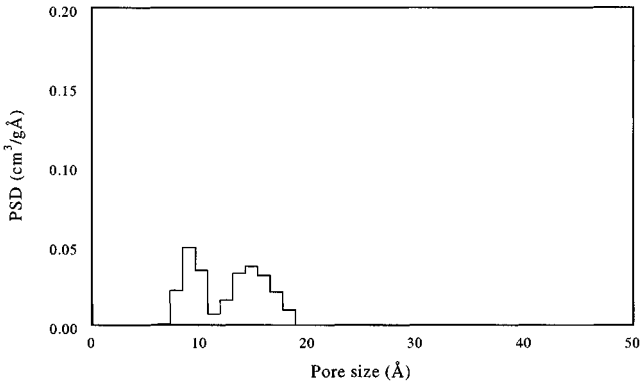

Figure 6. PSD for AC40 activated carbon based on the adsorption of ethane at 293 K.

a wide range of adsorption. In particular, the PSD can be used to predict the pure-component adsorption of ethane and methane over a range of temperatures and pressures. Similarly, it can be used to predict the adsorption from binary mixtures of ethane and methane. Although we have only presented predictions of adsorption from binary mixtures at a single temperature and pressure due to a lack of experimental data with which to make a comparison, similar predictions can be made over a much larger range.

To investigate the effect of the window of reliability on the accuracy of the adsorption predictions we have calculated a PSD for the Nuxit activated carbon based on the ethane adsorption at a higher temperature, 363 K, and another using methane adsorption at 293 K. Figure 12 presents two PSDs based on the adsorption of ethane at 363 K. Two PSDs are presented because the optimal smoothing parameters based on GCV and an *L* curve, which are usually in close agreement, are significantly different in this case. As expected, the PSD with the smaller smoothing parameter is more fragmented. The window of reliability for ethane adsorption at

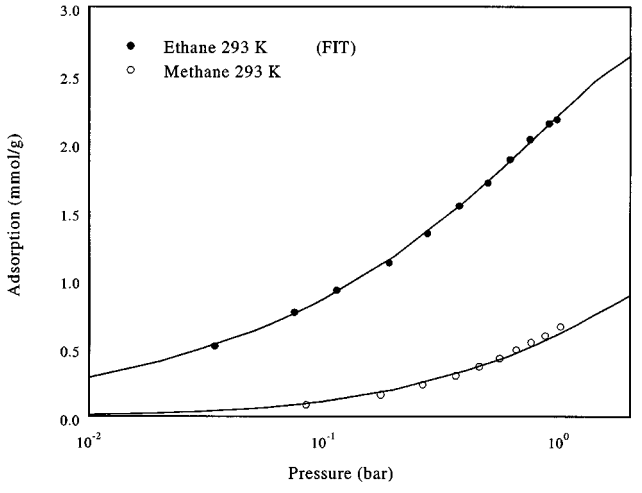

Figure 7. Predicted adsorption of methane at 293 K onto AC40 activated carbon based on the PSD in Figure 6 vs. experimental data.

Also shown is the fit to the ethane adsorption data at 293 K used to calculate the PSD.

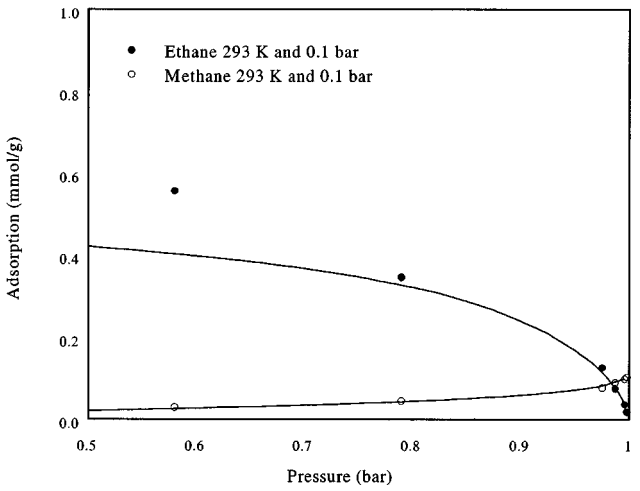

Figure 8. Predicted adsorption from bulk fluid mixtures at 293 K and 0.1 bar onto AC40 activated carbon based on the PSD in Figure 6 vs. experimental data.

363 K is slightly smaller than those of the ethane adsorption at 293 K and 313 K. (The windows of reliability are listed in Table 2.) This means a PSD based on the ethane adsorption at 363 K will not be able to differentiate between some of the larger pore sizes that are important for the adsorption of ethane at the higher pressures at 293 K and 313 K. Comparison of Figure 12 with Figure 3, which shows the Nuxit PSD at 293 K, shows that the PSDs calculated at the two temperatures are similar below the upper limit of the window of reliability at the higher temperature (363 K), and significantly different outside the window of reliability.

This inability to differentiate the largest pore sizes can be seen by comparing Figure 12 to Figure 3. The peak in Figure 3 that lies between 22 to 30 Å has effectively been subsumed into the last peak of each PSD presented in Figure 12. The effect of this on predicting adsorption can be seen in Figure 13 and Figure 14. (In these figures, the predictions based on both PSDs are shown only for the adsorption of pure ethane at 293 K, where there are some differences at high pressures. Since the predictions based on the two PSDs are virtually

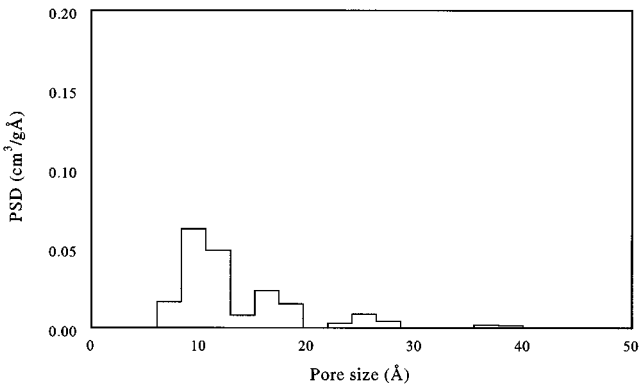

Figure 9. PSD for AK activated carbon based on the adsorption of ethane at 303 K.

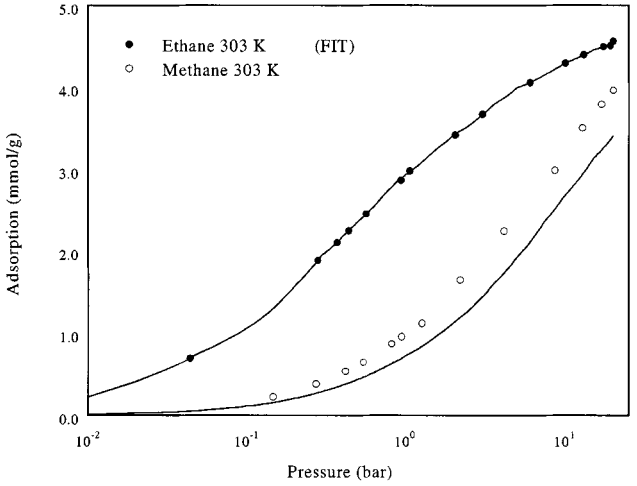

Figure 10. Predicted adsorption of methane at 303 K onto AK activated carbon based on the PSD in Figure 9 vs. experimental data.

Also shown is the fit to the ethane adsorption data at 303 K that was used to calculate the PSD.

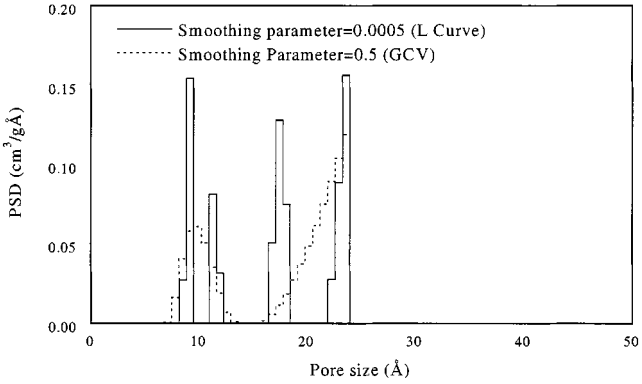

Figure 12. Two PSDs for Nuxit activated carbon based on the adsorption of ethane at 363 K.

The two PSDs correspond to two significantly different optimal smoothing parameters that were identified using generalized cross validation and an *L* curve.

identical for the remaining conditions, only the predictions based on the *L* curve PSD have been presented.) The window of reliability exceeds 24 Å for the ethane adsorption at 293 K and 313 K for pressures above 4 bar and 5 bar, respectively, that is, above these pressures significant adsorption occurs in a range of the PSD that was not accounted for in the PSD analysis using ethane at 363 K. As expected, the reliability of the predictions presented in Figure 13 deteriorates above these pressures.

Figure 15 presents the PSD for Nuxit activated carbon based on methane adsorption at 293 K. In this case, the window of reliability only extends to 20 Å. This window is exceeded above pressures of 0.5 bar, 1 bar, 2 bar, and 2.5 bar for the adsorption of ethane at 293 K, 313 K, 333 K, and 363 K, respectively. As before, Figures 16 and 17 show that predictions in regions that do not lie within the window of reliability (determined by the temperature, pressure, and identify of the adsorption species) are significantly in error.

The PSD for the Nuxit activated carbon presented in Figure 3 has a higher resolution (that is, the quadrature intervals are smaller) compared to the PSDs for either the AC40 or AK activated carbons presented in Figure 6 and Figure 9. This is merely a consequence of the fact that the isotherm

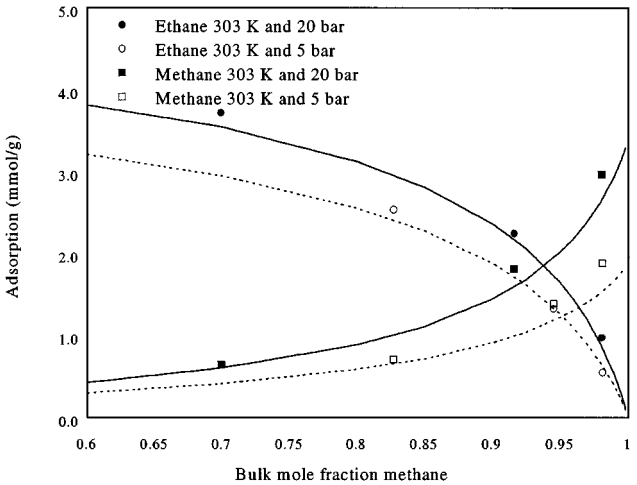

Figure 11. Predicted adsorption from bulk fluid mixtures at 303 K and at 5 and 20 bar onto AK activated carbon based on the PSD in Figure 9 vs. experimental data.

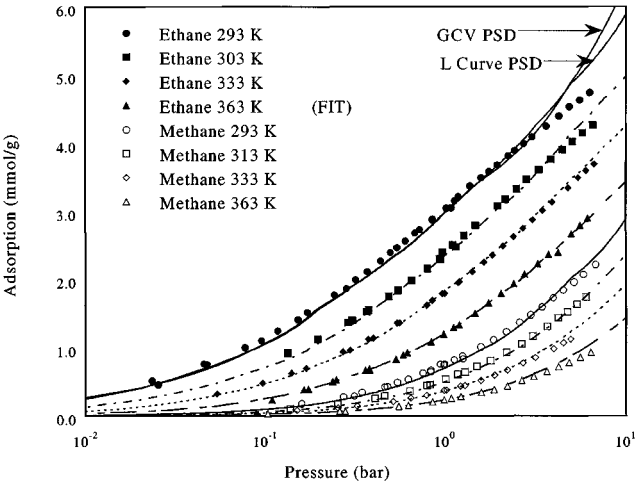

Figure 13. Predicted adsorption of ethane at 293, 313 and 333 K, and methane at 293, 313, 333 and 363 K onto Nuxit activated carbon based on the *L* curve PSD in Figure 12 vs. experimental data.

Predictions based on the GCV PSD were virtually identical for all the isotherms except for the adsorption of ethane at 293 K. Also shown is the fit to the ethane adsorption data at 363 K used to calculate the PSD.

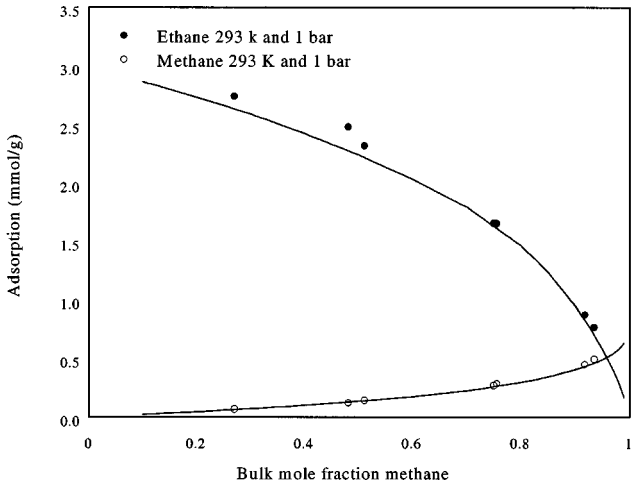

Figure 14. Predicted adsorption from bulk fluid mixtures at 293 K and 1 bar onto Nuxit activated carbon based on the *L* curve PSD vs. Figure 12 vs. experimental data.

Predictions based on the GCV PSD were virtually identical to those presented in this figure.

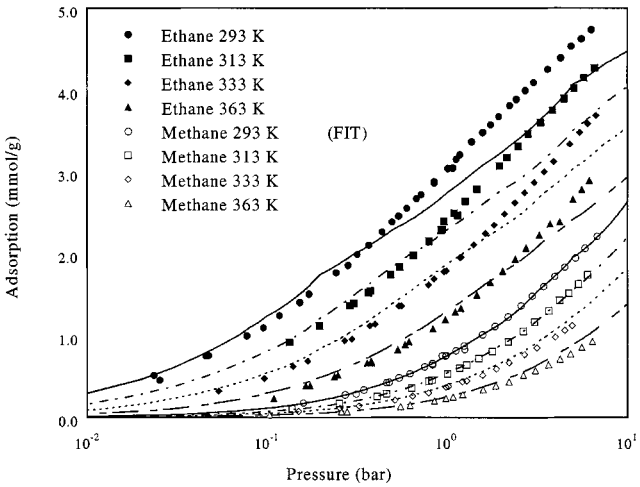

Figure 16. Predicted adsorption of ethane at 293, 313, 333 and 363 K, and methane at 313, 333 and 363 K onto Nuxit activated carbon based on the PSD in Figure 15 vs. experimental data.

Also shown is the fit to the methane adsorption data at 293 K used to calculate the PSD.

used to calculate the Nuxit PSD contained significantly more data points than the isotherms for the other two activated carbons. To determine whether the resolution of the PSD is an important factor when predicting adsorption, we calculated three PSDs for the Nuxit activated carbon based on 9, then 5, and finally only 3 of the original 39 pure component ethane adsorption data points at 293 K. These data are summarized in Table 3, and the resulting PSDs are presented in Figure 18. Note that since in each case we included the adsorption data point at the highest pressure for this isotherm, the windows of reliability extend, as before, from 6.1 Å to 30 Å. Quite surprisingly, the predictions based on all three PSDs presented in Figure 18 are only marginally worse than those presented in Figures 4 and 5. The worst of these, which are the predictions based on the PSD calculated from only three data points, are presented in Figure 19 and Figure 20. Similar results were observed for the AC40 and AK activated carbons. In particular, predictions not significantly different from those presented in Figure 7 and Figure 8 could be made from a PSD based on only three data points for the AC40 activated carbon. Equally, predictions of comparable accuracy to those presented in Figures 10 and 11 for the adsorption onto AK activated carbon could be made from a PSD based on four data points. These results are a strong indication that the resolution of a PSD is much less important than the size of the window of reliability when predicting adsorption. This is in contrast to the situation illustrated in Figure 2, in which the alternative PSDs are detailed, but with a narrow window

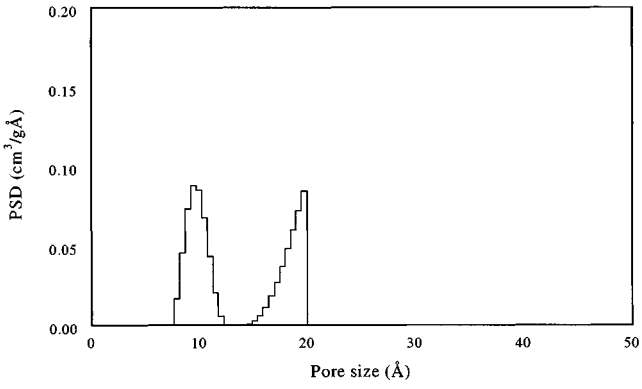

Figure 15. PSD for Nuxit activated carbon based on the adsorption of methane at 293 K.

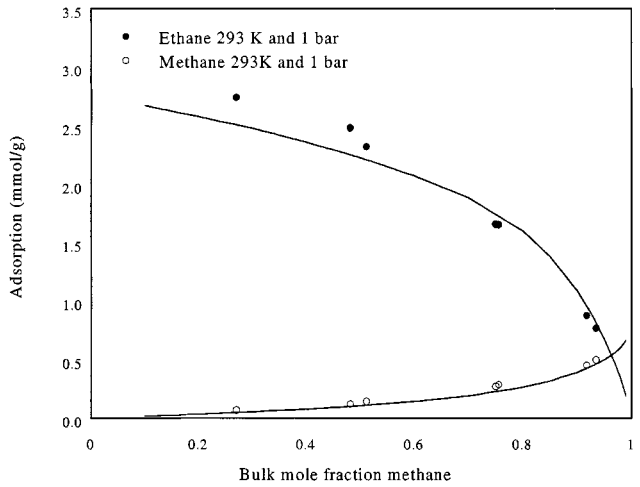

Figure 17. Predicted adsorption from bulk fluid mixtures at 293 K and 1 bar onto Nuxit activated carbon based on the PSD in Figure 15 vs. experimental data.

Table 3. Data Points of the Ethane Adsorption Isotherm at 293 K onto Nuxit Activated Carbon Used to Determine the Effect of the PSD Resolution on Predictions of Adsorption

Pressure (bar)	Adsorption (mmol/g)	PSD 9 points	PSD 5 points	PSD 3 points
0.006	0.229	√	√	√
0.023	0.514			
0.025	0.456			
0.046	0.757	√		
0.047	0.754			
0.077	1.000			
0.095	1.099			
0.118	1.244			
0.152	1.408	√	√	
0.172	1.510			
0.243	1.765			
0.285	1.861			
0.320	1.989			
0.371	2.105	√		
0.440	2.266			
0.501	2.387			
0.543	2.460			
0.605	2.556			
0.683	2.675	√	√	
0.726	2.722			√
0.851	2.881			
0.852	2.866			
1.020	3.045			
1.080	3.049	√		
1.133	3.156			
1.183	3.211			
1.377	3.373			
1.584	3.487			
1.752	3.580	√	√	
1.943	3.679			
2.231	3.814			
2.420	3.887			
2.728	3.996			
3.033	4.091	√		
3.620	4.250			
4.262	4.394			
4.875	4.529			
5.553	4.624			
6.318	4.736	√	√	√

Source: Szepesy and Illes (1963a,b,c).

of reliability; in that case, significant ethane adsorption occurs above the window of reliability of the PSD (obtained using methane), and the prediction of ethane adsorption is therefore poor.

Before progressing to the next section, it is worth noting a technical aspect of calculating PSDs based on so few data points. In this case, both the GSV and *L*-curve methods that are used to identify the optimal smoothing parameter fail. This occurs because it becomes impossible to calculate numerical approximations to the second derivative of the PSD. Fortunately, however, including so few data points in the analysis in itself acts as a smoothing mechanism and stabilizes the calculation. Smoothing is therefore redundant for a PSD analysis with only a few data points.

Predicting Adsorption Based on Adsorption Data of More Than One Component

When investigating a chosen activated carbon for an industrial application there might be more than one pure-component adsorption isotherm available for that carbon. Some multicomponent adsorption data might also be available, although given the high cost of multicomponent adsorption equilibrium measurements, such data are unlikely to be extensive. Equation 1, applied in the previous section to adsorption of a pure component, can also be used to obtain a PSD on the basis of a range of pure-component and multicomponent data. Including additional data has two direct impacts on the analysis. First, as we saw in the previous section,

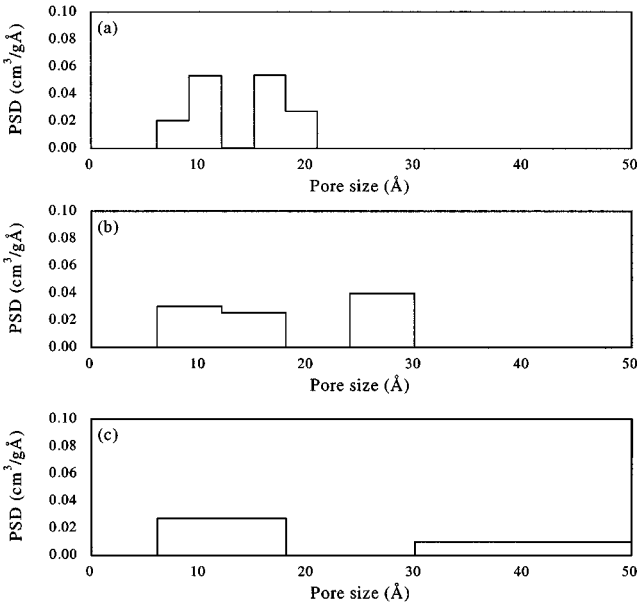

Figure 18. PSDs for Nuxit activated carbon based on (a) 9, (b) 5, and (c) 3 of the original 39 data points in the ethane isotherm at 293 K.

The actual data used are presented in Table 3.

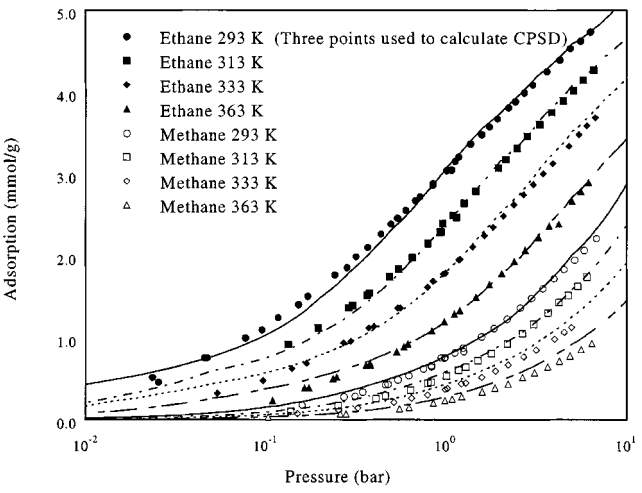

Figure 19. Predicted adsorption of ethane at 293, 313, 333 and 363 K, and methane at 293, 313, 333 and 363 K onto Nuxit activated carbon vs. experimental data.

The predictions are based on the PSD presented in Figure 18c.

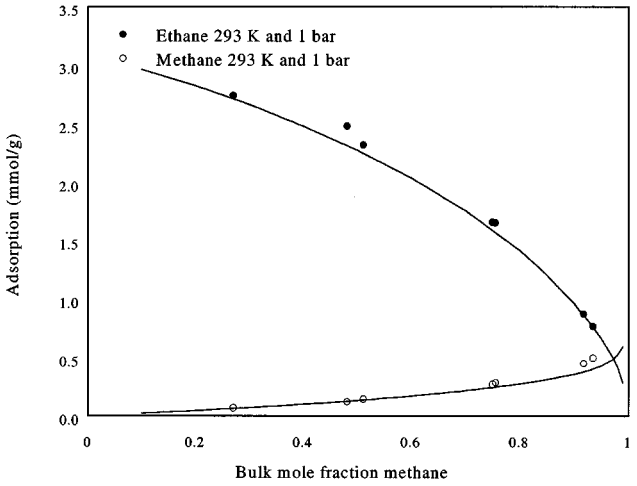

Figure 20. Predicted adsorption from bulk fluid mixtures at 293 K and 1 bar onto Nuxit activated carbon vs. experimental data.

The predictions are based on the PSD presented in Figure 18c.

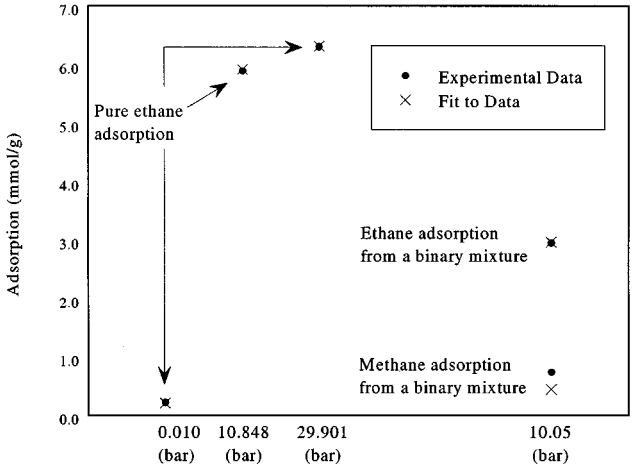

Figure 22. Fit to a limited amount of pure-component and binary adsorption data onto BPL activated carbon.

additional data improves the resolution of the resulting PSD. However, the results of the previous section revealed that the resolution of the PSD has only a small impact on the accuracy of the adsorption predictions. The second impact, which is significantly more useful than the first, is concerned with the inherent suitability of modeling the internal structure of an activated carbon as a collection of model pores with no connectivity effect, that is, a conventional PSD.

As more data are included in the analysis, so the credibility of the resulting PSD (provided it fits the data well) increases. In the Introduction we noted that it has been shown that some activated carbons, BPL being an example, cannot be modeled using a conventional PSD (Davies and Seaton, 1999). Of particular significance from this previous investigation is the fact that at least some binary adsorption data were required in order to establish that a PSD is an inappropriate

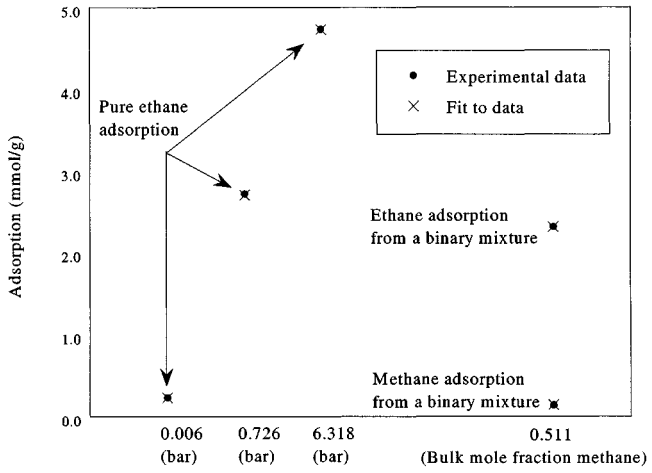

Figure 21. Fit to a limited amount of pure-component and binary adsorption data onto Nuxit activated carbon.

model for the internal structure of BPL activated carbon. Therefore, although the results of the previous section show that excellent predictions can often be made using a PSD obtained from a single pure-component isotherm, this is not guaranteed. To calculate a PSD that can be used to predict adsorption *with a high degree of confidence* would therefore require (1) a limited amount of pure-component adsorption data spanning a suitable window of reliability, and (2) a limited amount of multicomponent data.

As already indicated in the Introduction, the ''high degree of confidence'' just described cannot in general be attained for predictions based on a classical thermodynamic method such as IAST. This is due to the fact that the validity of these methods can be determined only by comparing predicted extents of adsorption to some multicomponent adsorption data. To achieve this, however, we would require a complete set of pure-component isotherms and some multicomponent adsorption data, all at the temperature of interest. These data requirements are particularly severe. In contrast, a GCMC/PSD analysis can utilize any multicomponent data that is available to establish the suitability of the analysis. Compared with classical thermodynamic models such as IAST, the total data requirements for the GCMC/PSD analysis are extremely modest: the pure-component and multicomponent adsorption data do not necessarily need to be at the same temperature, none of the data need be at the temperature of the required predictions, and the analysis does not require pure-component adsorption isotherms for all the components involved.

To demonstrate this concept, suppose we wish to predict the binary adsorption of methane and ethane onto Nuxit and BPL activated carbon at 333 K. IAST would only be capable of making such predictions if we had access to the pure-component methane and ethane isotherms for each carbon at 333 K. Further, without any prior information, the only way to determine the reliability of these predictions would be to compare them to some binary adsorption data for each carbon at 333 K. In contrast, predictions based on a GCMC/PSD analysis would only require a few pure-component adsorp-

tion measurements for each carbon (at any temperature) and any available binary adsorption data could be used to check the reliability of the predictions. For example, using the three ethane adsorption measurements onto Nuxit activated carbon at 293 K identified in Table 3 and one or more of the binary adsorption measurements, available at 293 K and 1 bar, shows that a highly consistent PSD could be calculated for this carbon. The excellent fit to these data points is presented in Figure 21. Therefore, it is reasonable to place a fair degree of confidence in predictions based on this PSD. In constrast, by attempting to fit a PSD to three ethane adsorption measurements at 308 K onto BPL activated carbon and a single binary adsorption measurement, such as the adsorption at 373 K and 10 bar, would reveal that no PSD consistent with the data exists. This can be deduced because it is not possible to accurately fit the binary methane adsorption data, as shown in Figure 22. Considering that so few data points have been used to fit the PSD, we should expect excellent agreement (since it is easier to fit a function, in this case the PSD, to only a few data points). Hence, any predictions based such a characterization are likely to fail catastrophically.

Being unable to fit a PSD to a given set of experimental data is direct evidence that at least one important attribute of the activated carbon that has a significant effect on adsorption is being omitted from the characterization. When this occurs, as in the case of BPL activated carbon, it is worth considering more refined models of the internal structure. An incrementally more refined model of the internal structure is one that takes the pore network connectivity into account [see, for example, López-Ramón et al. (1997) and Davies and Seaton (1999)]. This model explicitly makes allowance for the fact that some components may only be able to adsorb within part of the adsorbent due to bottlenecks in the structure. The accessibility of species l, A_l, is defined by

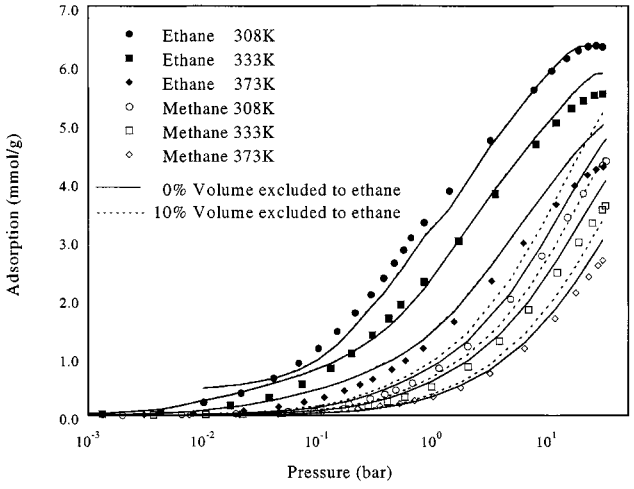

Figure 23. Predicted adsorption of ethane at 308, 333 and 373 K, and methane adsorption at 308, 333, and 373 K onto BPL activated carbon vs. experimental data.

The predictions are based on PSDs calculated using three ethane adsorption measurements at 308 K, a binary adsorption measurement at 373 K and 10 bar, and an ethane accessibility of 100 and 90%.

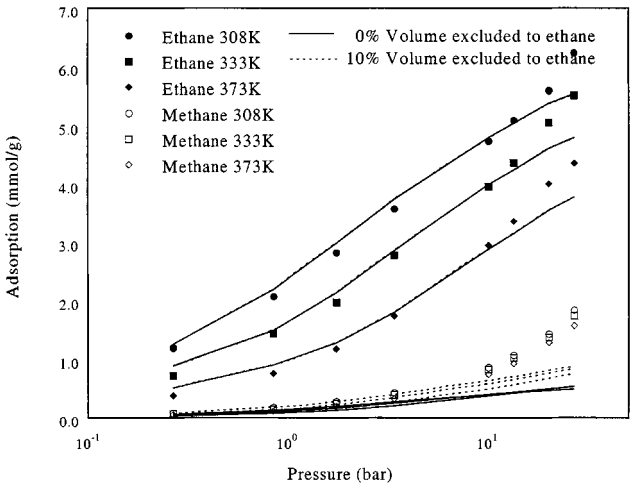

Figure 24. Predicted adsorption from a 50:50 methane: ethane bulk-gas mixture at 308, 333 and 373 K onto BPL activated carbon vs. experimental data.

The two PSDs were calculated as described in Figure 23.

$$A_l = \frac{\text{Number of pores into which component } l \text{ can enter}}{\text{Number of pores that are large enough to accommodate component } l}. \quad (4)$$

As we have shown previously (Davies and Seaton, 1999), Eq. 1 can be extended to include accessibilities:

$$N_s(T, f)_i = \sum_{i=s}^{k} (A_l - A_{l+1}) \int_0^\infty \rho_{mp,s}(w, T, f_l)_i f(w)\, dw \qquad l = 1 \cdots n, \quad (5)$$

where $N_s(T, f)_i$ is the adsorption of a species s from a bulk gas phase consisting of k components; f is a vector of fugacities of the k components; $\rho_{mp,s}(w, T, f_l)_i$ is the adsorption of species s within a region available to the first l components; and $f(w)$ is the PSD. [For clarity, we point out that the "accessibility" used in this work is not directly comparable to that of López-Ramón et al. (1997).]

To demonstrate the potential improvements that can be made by using these models, Figures 23 to 25 compare predicted extents of binary methane and ethane adsorption onto BPL based on ethane having 100 and 90% accessibility to the pore volume. The pore-size distributions used in these predictions were based on three ethane adsorption measurements at 308 K and a single binary adsorption measurement at 373 K and 10 bar.

Although the predictions of binary adsorption shown in Figures 24 and 25 improve as the accessibility to ethane decreases, there are still significant discrepancies at high pressure. Significantly, these discrepancies are not reduced by calculating PSDs based on more experimental data. This is in agreement with our previous study (Davies and Seaton, 1999) that showed that although PSD analyses that include connectivity are significantly more realistic, they still seem to omit at

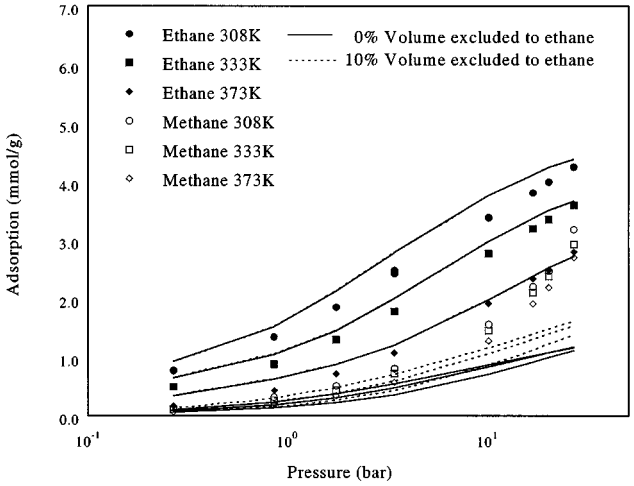

Figure 25. Predicted adsorption from a 75:25 methane: ethane bulk-gas mixture at 308, 333 and 373 K onto BPL activated carbon vs. experimental data.

The two PSDs were calculated as described in Figure 23.

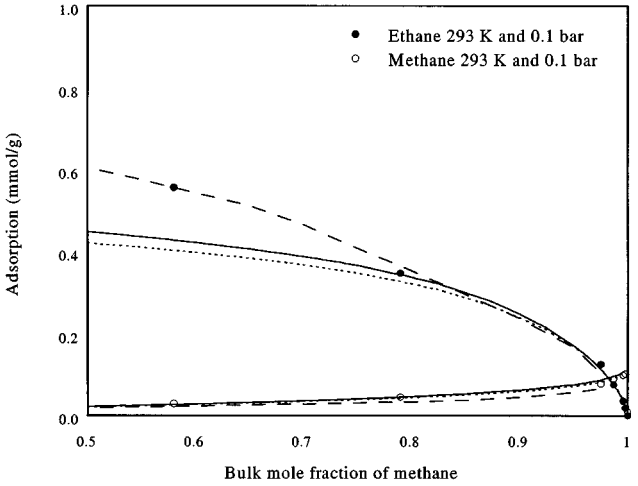

Figure 27. Predictions of the binary adsorption onto AC40 activated carbon of ethane and methane at 293 K and 0.1 bar vs. experimental data.

The broken line shows the predictions based on IAST, the dotted line the predictions based on a PSD calculated from the ethane adsorption at 293 K, and the solid line shows the predictions based on a PSD calculated from both the ethane and methane adsorption at 293 K.

least one important attribute of BPL that affects adsorption. Continued efforts in model development are, however, likely to improve this situation.

This concept of model development represents another distinct advantage of GCMC/PSD analyses over classical thermodynamic techniques. When classical thermodynamic techniques such as IAST fail, any improvements, such as introducing activity coefficients into the analysis, which is then termed real adsorbed solution theory (RAST) (Myers and Prausnitz, 1965), yield little physical insight and are even more data intensive than IAST. For example, RAST requires substantial binary adsorption data in order to evaluate the activity coefficients. Similar problems are encountered with the vacancy solution model (VSM) of Suwanayuen and Danner (1980). In contrast, developing improved models of the pore structure provides us with valuable information about the attributes of adsorbents that affect adsorption.

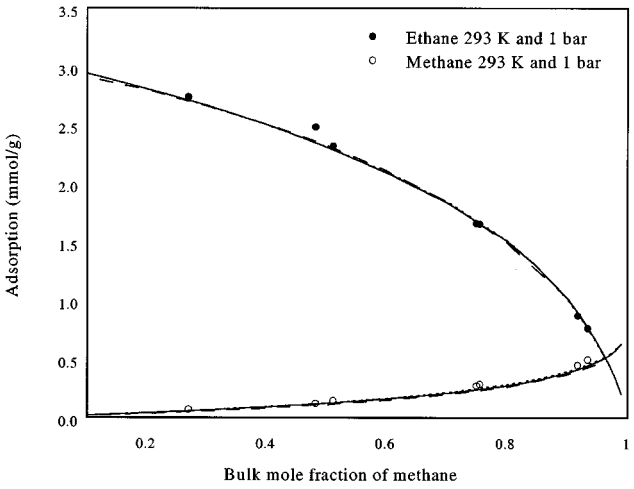

Figure 26. Predictions of the binary adsorption onto Nuxit activated carbon of ethane and methane at 293 K and 1 bar vs. experimental data.

The broken line shows predictions based on IAST, the dotted line predictions based on a PSD calculated from the ethane adsorption at 293 K, and the solid line shows predictions based on a PSD calculated from ethane and methane adsorption at 293 K.

We have compared GCMC/PSD predictions of adsorption onto Nuxit, AC40, and AK activated carbon directly to those of IAST. These results are presented in Figures 26 to 29. The predictions calculated using the GCMC/PSD approach were based on two PSDs: one based on only the pure-component ethane isotherm corresponding to the temperature of the mixture, and the other based on both the pure-component methane and ethane adsorption isotherms corresponding to the temperature of the mixture. Three aspects concerning these results are worth noting. First, the predictions that are based on the PSD calculated using the two pure-component isotherms utilize as much input data as IAST. However, these predictions are only marginally better than those calculated from the PSD based on a single pure-component isotherm. Further, the results of the previous section showed that similar results could be obtained using only three or four experimental data points. Second, the IAST predictions in these figures do not always cover the entire range of experimental conditions. This is because IAST is incapable of making predictions in these regions based on the available experimental data. Last, only in one instance, shown in Figure 27, does IAST lead to a significantly better prediction of multicomponent adsorption. It is worth noting that the window of reliability of the PSD of the AC40 carbon is fairly narrow and is

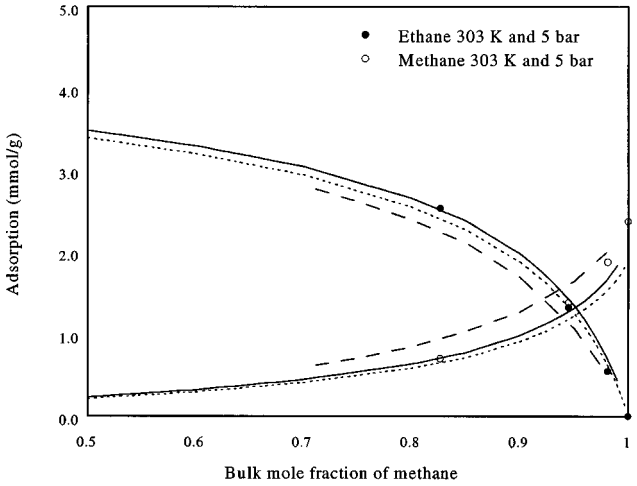

Figure 28. Predictions of the binary adsorption onto AK activated carbon of ethane and methane at 303 K and 5 bar vs. experimental data.

The broken line shows predictions based on IAST, the dotted line predictions based on a PSD calculated from the ethane adsorption at 303 K, and the solid line shows the predictions based on a PSD calculated from ethane and methane adsorption at 303 K.

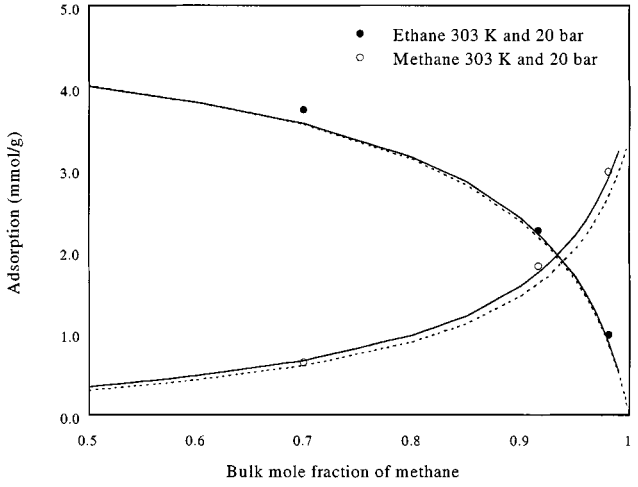

Figure 29. Predictions of the binary adsorption onto AK activated carbon of ethane and methane at 293 K and 1 bar vs. experimental data.

The dotted line shows the predictions based on a PSD calculated from the ethane adsorption at 303 K, and the solid line shows the predictions based on a PSD calculated from both the ethane and methane adsorption at 303 K.

most likely to be the reason for the discrepancy at 0.58 mol fraction of methane.

In summary, these results indicate that the GCMC/PSD method gives a similar accuracy to IAST, but with a greatly reduced requirement for experimental data.

Selecting and Designing Adsorbents Using the GCMC/PSD Method

As we indicated in the Introduction, because molecular simulation relates pore structure to adsorption, the GCMC/PSD method has potential as a design tool for adsorbents, as well as for adsorptive separation processes. The quality of the predictions demonstrated in the previous two sections support this proposition. In this section, we consider applying the GCMC/PSD method to three distinct modes of adsorbent design and selection:

1. Selecting an adsorbent for a particular industrial process, from among an existing set of candidate adsorbents;
2. Designing new adsorbents from scratch (that is, designer adsorbents);
3. Designing improved adsorbents based on existing adsorbents.

In the adsorbent selection problem, some experimental data would almost certainly be available for the set of candidate adsorbents. These data might not be for adsorptive species involved in the target application, but they could nevertheless be used to characterize the pore structure. In the case of an activated carbon adsorbent, Eq. 1 would be used to obtain the PSD. A standard adsorption characterization experiment, such as the adsorption of nitrogen at 77 K, might be used. Alternatively, adsorption data for another species, perhaps more similar to the species involved in the industrial application, might be used. (The advantage of the latter approach is that one is making a smaller extrapolation in, for example, predicting the adsorption of propane based on a PSD determined using ethane at close to ambient temperature, than in using a PSD obtained using nitrogen at 77 K.) Clearly, other types of adsorbent would require different characterization data; for example, in the case of a zeolite, information on the cation distribution would be needed from some experimental source.

Engineering designer adsorbents (that is, designing an adsorbent from scratch for a particular application) is closely related to the techniques that can be employed to manufacture the new adsorbent. For example, a recent technique that aims at producing an activated carbon with relatively uniform slit-shaped pores employs a pillared clay as a template [see, for example, Sonobe et al. (1988), and Bandosz et al. (1995)]. If this technique is eventually refined to the state where it is possible to vary the pore size using different pillared clays or processing techniques, then it would be most helpful to be able to calculate the best pore size to attempt to synthesize for a proposed separation. Pore-network models, in conjunction with molecular simulations, are ideally suited to perform these calculations. Similarly, these tools can be used to design an optimal adsorbent structure that can be employed as an alternative method to store gases in preference to high-pressure storage cylinders. Calculations that investigated the effect of pore size, pore-wall thickness, and pore geometry have recently been performed by Cracknell et al. (1993), Kefer et al. (1996a,b), Suzuki et al. (1996), Chen et al. (1997), McEnaney et al. (1998), Yin et al. (1998), and Wang and Johnson (1999).

Many new adsorbents are, however, based on improvements to existing adsorbents. For example, activated carbons with differing pore structure can be obtained from a given precursor by varying the processing conditions. The techniques used to produce improved adsorbents invariably involve trial-and-error modifications to the processing stages

that are required in the manufacture of the activated carbon. GCMC/PSD analyses are ideally suited to limit the extent of the trial-and-error search. This can be achieved by reliably characterizing the original adsorbent. As discussed in the previous section, in order to characterize the internal structure of an activated carbon using a PSD and to ensure that such a characterization is reliable will invariably require some pure-component and multicomponent adsorption data. Once the adsorbent has been characterized, potential modifications to the pore structure can be investigated directly using GCMC simulation. For example, the effect of increasing the average pore size on the separation performance or storage capacity can be investigated. Note that in evaluations such as these, a hypothetical adsorbent is being generated and its performance is being assessed without actually having to manufacture the adsorbent. Once the attributes that are most likely to lead to the greatest overall improvement to the original adsorbent's performance have been identified, then the trial-and-error modifications in the processing stages can be directed to specifically achieving the desired modifications to the structure.

Conclusions

We have demonstrated that the GCMC/PSD method is capable of accurately predicting pure-component and mixture adsorption over a wide range of conditions, using only a limited set of data to obtain the PSD.

The agreement with experiment is similar in quality to that of the standard classical thermodynamic method, IAST, but the requirement for experimental data is substantially smaller. Whereas classical thermodynamic models require as inputs detailed pure-component isotherms over the temperature range of interest, the GCMC/PSD analysis can predict a wide range of pure and multicomponent adsorption based on as little as three to four pure-component data points. This suggests that for mixtures of light hydrocarbons on activated carbon, the GCMC/PSD method is more economical than classical thermodynamic methods.

The GCMC/PSD approach also offers a much greater flexibility with respect to the type of adsorption data on which to base predictions compared to classical thermodynamic models. The adsorption data used to calculate the PSD do not need to be measured at the temperature of the required predictions and, if any multicomponent data exist, they can readily be incorporated into the analysis, improving the confidence that can be placed in the predictions.

The predictive ability of the GCMC/PSD method is based on identifying and quantifying the important characteristics of activated carbons that affect their adsorption behavior. Notably, these characteristics are at the molecular and pore levels, and allow us to harness the power of a statistical mechanical method to predict a wide range of adsorption behavior.

Another advantage of the GCMC/PSD method is that, where the description of the pore structure in terms of a PSD alone fails, the method can be systematically modified to incorporate other attributes of the internal structure. In our study of adsorption onto BPL activated carbon, we incorporated a measure of pore network connectivity into the characterization. Other properties, such as surface roughness or chemical heterogeneity, could be incorporated in a similar way. This is another point of distinction between a statistical mechanical method, such as GCMG simulation, and classical thermodynamic methods where there is no rigorous mechanism for incorporating refinements at the pore level.

We have found that the most significant factor that affects the accuracy of the GCMC/PSD predictions is the window of reliability. Predictions that do not lie within the window of reliability of the data points used to calculate the PSD are unlikely to be accurate. In contrast to the importance of the window of reliability, the resolution of the PSD seems to have little effect on the accuracy of the predicted extents of adsorption. This surprising result suggests that only a few adsorption data, spanning a suitable window of reliability, are required in order to calculate a PSD that can be used to predict adsorption.

The fact that we have found that good predictions of adsorption can often be made using the PSD of real adsorbents suggests that the GCMC/PSD method can also be used as a tool to design adsorbents.

Finally, we suggest that although we have demonstrated the power of the GCMC/PSD method only for light hydrocarbons on carbon adsorbents, the approach has potential to describe other systems. Heuchel et al. (1999) have shown that the GCMC method can describe the adsorption of methane/carbon dioxide on carbon (that is, a mixture of a nonpolar species and a quadrupolar species, still on a largely nonpolar adsorbent). The adsorption of mixtures of nonpolar and dipolar species (such as organics/water) on carbon, involves an extra dimension—the polarity of the surface (Muller et al., 1996; McCallum et al., 1999) in addition to the PSD and, if necessary, pore-network connectivity. The GCMC/PSD method might also be applicable to other noncrystalline adsorbents such as silica gel.

Acknowledgments

G. M. Davies gratefully acknowledges financial support from the Bradlow Foundation. The donors of The Petroleum Research Fund, administered by the ACS, are acknowledged for partial support of this work. We also thank V. Y. Gusev for helpful comments during the preparation of this article.

Literature Cited

Allen, M. P., and D. J. Tildesley, *Computer Simulation of Liquids,* Oxford Science Publ., Oxford (1987).

Bandosz, T. J., K. Putyera, J. Jagiello, and J. A. Schwarz, ''Hydrotalcite-Like Structures as Molecular Containers for Preparation of Microporous Carbons,'' *Appl. Clay Sci.*, **10**, 177 (1995).

Chen, X. S., B. McEnaney, T. J. Mays, J. Alcaniz-Monge, D. Cazorla-Amoros, and L. Linares-Solano, ''Theoretical and Experimental Studies of Methane Adsorption on Microporous Carbons,'' *Carbon*, **35**, 1251 (1997).

Costa, E., J. L. Sotelo, G. Calleja, and C. Marron, ''Adsorption of Binary and Ternary Hydrocarbon Gas Mixtures on Activated Carbon,'' *AIChE J.*, **27**, 5 (1981).

Cracknell, R. F., and D. Nicholson, ''Grand-Canonical Monte-Carlo Study of Lennard-Jones Mixtures in Slit Pores: 3. Mixtures of 2 Molecular Fluids—Ethane and Propane,'' *J. Chem. Soc.—Faraday Trans.*, **90**, 11, 1487 (1994).

Cracknell, R. F., P. Gordon, and K. E. Gubbins, ''Influence of Pore Geometry on the Design of Microporous Materials for Methane Storage,'' *J. Chem. Phys.*, **97**, 494 (1993).

Davies, G. M., and N. A. Seaton, ''Development and Validation of Pore Structure Models for Adsorption in Activated Carbons,'' *Langmuir*, **15**, 6263 (1999).

Davies, G. M., N. A. Seaton, and V. S. Vassiliadis, ''Calculation of Pore Size Distributions of Activated Carbons from Adsorption Isotherms,'' *Langmuir*, **15**, 8235 (1999).
Frenkel, D., and B. Smit, *Understanding Molecular Simulation*, Academic Press, San Diego (1996).
Gregg, S. J., and K. S. W. Sing, *Adsorption, Surface Area and Porosity*, Academic Press, London (1982).
Gusev, V. Y., and J. A. O'Brien, ''Can Molecular Simulation be Used to Predict Adsorption on Activated Carbons?,'' *Langmuir*, **13**, 2822 (1997).
Gusev, V. Y., J. A. O'Brien, and N. A. Seaton, ''A Self-Consistent Method for Characterization of Activated Carbons Using Supercritical Adsorption and Grand Canonical Monte-Carlo Simulations,'' *Langmuir*, **13**, 2815 (1997).
Gusev, V. Y., J. A. O'Brien, C. R. C. Jensen, and N. A. Seaton, ''Theory for Multicomponent Adsorption Equilibrium: Multispace Adsorption Model,'' *AIChE J.*, **42**, 2773 (1996).
Heuchel, M., G. M. Davies, E. Buss, and N. A. Seaton, ''Adsorption of Carbon Dioxide and Methane and Their Mixtures on an Activated Carbon: Simulation and Experiment,'' *Langmuir*, **15**, 8695 (1999).
Hirschfelder, J. O., C. F. Curtiss, and R. B. Bird, *Molecular Theory of Gases and Liquids*, Wiley, New York (1954).
Keffer, D., H. T. Davis, and A. V. McCormick, ''The Effect of Nanopore Shape on the Structure and Isotherms of Adsorbed Fluids,'' *Adsorption J. Int. Adsorption Soc.*, **2**, 9 (1996a).
Keffer, D., H. T. Davis, and A. V. McCormick, ''Effect of Loading and Nanopore Shape on Binary Adsorption Selectivity,'' *J. Phys. Chem.*, **100**, 638 (1996b).
López-Ramón, M. V., J. Jagiello, T. J. Bandosz, and N. A. Seaton, ''Determination of the Pore Size Distribution and Network Connectivity in Microporous Solids by Adsorption Measurements and Monte Carlo Simulation,'' *Langmuir*, **13**, 4435 (1997).
McCallum, C. L., T. J. Bandosz, S. C. McGrother, E. A. Muller, and K. E. Gubbins, ''A Molecular Model for Adsorption of Water on Activated Carbon: Comparison of Simulation and Experiment,'' *Langmuir*, **15**, 533 (1999).
McEnaney, B., T. J. Mays, and X. Chen, ''Computer Simulations of Adsorption Processes in Carbonaceous Adsorbents,'' *Fuel*, **77**, 557 (1998).
Merz, P. H., ''Determination of Adsorption Energy Distribution by Regularization and a Characterization of Certain Adsorption Isotherms,'' *J. Comput. Phys.*, **38**, 64 (1980).
Muller, E. A., L. F. Rull, L. F. Vega, and K. E. Gubbins, ''Adsorption of Water on Activated Carbons: A Molecular Simulation Study,'' *J. Phys. Chem.*, **100**, 1189 (1996).
Myers, A. L., and J. M. Prausnitz, ''Thermodynamics of Mixed-Gas Adsorption,'' *AIChE J.*, **11**, 121 (1965).
Nicholson, D., and N. G. Parsonage, *Computer Simulation and the Statistical Mechanics of Adsorption*, Academic Press, London (1982).
Richter, E., W. Schutz, and A. L. Myers, ''Effect of Adsorption Equation on Prediction of Multicomponent Adsorption Equilibria by the Ideal Adsorbed Solution Theory,'' *Chem. Eng. Sci.*, **44**, 1609 (1989).
Sonobe, N., T. Kyotani, and A. Tomita, ''Formulation of Highly Orientated Graphite from Polyacrylonitrile by Using a Two-Dimensional Space Between Montmorillonite Lamellae,'' *Nature*, **331**, 331 (1988).
Steele, W. A., *The Interaction of Gases with Solid Surfaces*, Pergamon Press, Oxford (1974).
Suwanayuen, S., and R. P. Danner, ''Vacancy Solution Theory of Adsorption from Gas Mixtures,'' *AIChE J.*, **26**, 76 (1980).
Suzuki, T., K. Kaneko, N. Setoyama, M. Maddox, and K. Gubbins, ''Grand Canonical Monte Carlo Simulation for Nitrogen Adsorption in Graphitic Slit Micropores: Effect of Interlayer Distance,'' *Carbon*, **34**, 909 (1996).
Szepesy, L., and V. Illes, ''Adsorption of Gases and Gas Mixtures: I. Measurement of the Adsorption Isotherms of Gases on Active Carbon up to Pressures of 1000 Torr,'' *Acta Chim. Hung. Tomus*, **35**, 37 (1963a).
Szepesy, L., and V. Illes, ''Adsorption of Gases and Gas Mixtures: II. Measurement of the Adsorption Isotherms of Gases on Active Carbon Under Pressures of 1 to 7 Atm.,'' *Acta Chim. Hung. Tomus*, **35**, 53 (1963b).
Szepesy, L., and V. Illes, ''Adsorption of Gases and Gas Mixtures: III. Investigation of the Adsorption Equilibria of Binary Gas Mixtures,'' *Acta Chim. Hung. Tomus*, **35**, 245 (1963c).
Von Szombathely, M., P. Brauer, and M. Jaroniec, ''The Solution of Adsorption Integral Equations by Means of the Regularization Methods,'' *J. Comput. Chem.*, **13**, 17 (1992).
Wahba, G., ''Practical Approximate Solutions to Linear Operator Equations when the Data Are Noisy,'' *SIAM J. Numer. Anal.*, **14**, 651 (1982).
Wang, Q. Y., and J. K. Johnson, ''Computer Simulations of Hydrogen Adsorption on Graphite Nanofibers,'' *J. Phys. Chem. B*, **103**, 277 (1999).
Wilson, J. D., ''Statistical Approach to the Solution of First-Kind Integral Equations Arising in the Study of Materials and Their Properties,'' *J. Mater. Sci.*, **27**, 3911 (1992).
Yin, Y. F., T. Y. Mays, and B. McEnaney, ''Adsorption Potentials and Simulations in Carbon Slits and Cylinders,'' *Fundamentals of Adsorption: 6. Proceedings of the Sixth International Conference of Fundamental of Adsorption*, F. Meunier, ed., Elsevier, Amsterdam, p. 261 (1998).

Manuscript received Oct. 20, 1999, and revision received Mar. 27, 2000.